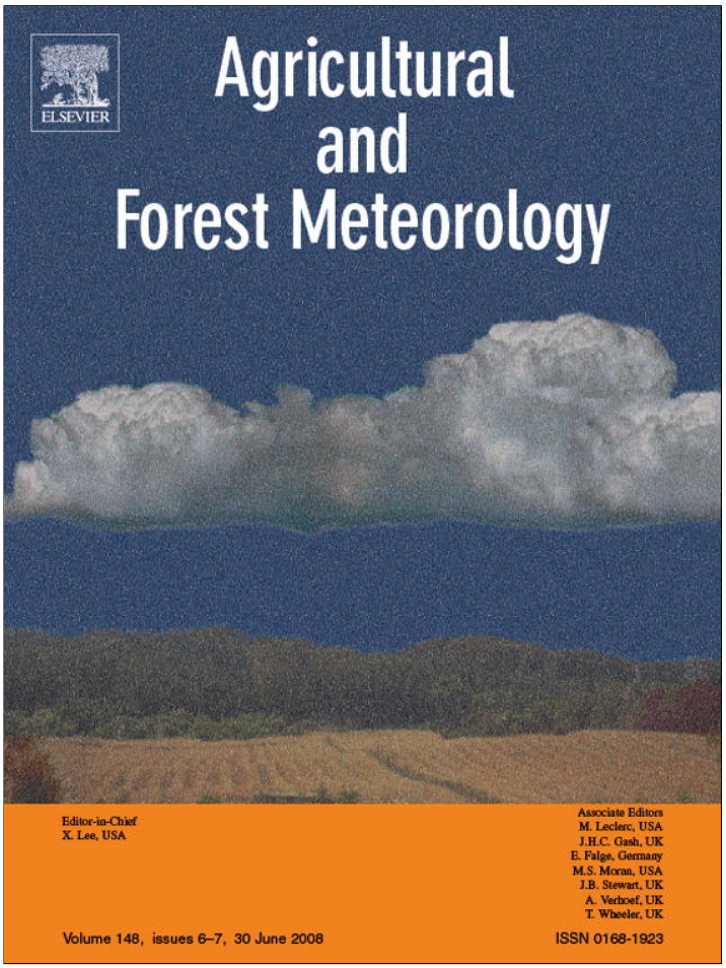

AGRICULTURAL AND FOREST METEOROLOGY 148 (2008) 1101–1108

available at www.sciencedirect.com

ScienceDirect

journal homepage: www.elsevier.com/locate/agrformet

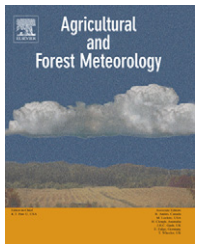

Analysis of photosynthetic photon flux density and its parameterization in Northern China

X. Xia [a,*], Z. Li [b], P. Wang [a], M. Cribb [b], H. Chen [a], Y. Zhao [c]

[a] LAGEO, Institute of Atmospheric Physics, Chinese Academy of Sciences, Beijing, China
[b] Department of Atmospheric and Oceanic Science and ESSIC, University of Maryland, Maryland, USA
[c] Chinese Academy of Meteorological Sciences, Chinese Meteorological Administration, Beijing, China

ARTICLE INFO

Article history:
Received 23 July 2007
Received in revised form
22 February 2008
Accepted 22 February 2008

Keywords:
Photosynthetic photon flux density
Aerosol
Water vapor
Clearness index
Parameterization

ABSTRACT

The relationship between broadband global solar radiation (R_S) and photosynthetic photon flux density (Q_P) is investigated using 2 year's worth of radiation data collected at a site in northern China. These data are used to determine the temporal and monthly variability of the ratio Q_P/R_S and its dependence on aerosol optical depth (AOD) and the column-integrated water vapor content. A simple and efficient all-weather empirically derived model is proposed to estimate Q_P from R_S. Results reveal that the monthly variation of the ratio Q_P/R_S ranges from 1.87 E MJ^{-1} in January to 2.08 E MJ^{-1} in July with an annual mean value of 1.96 E MJ^{-1}. Large day-to-day variations in aerosol loading resulted in large variations in Q_P/R_S. Under cloudless conditions, aerosols lead to a reduction of about 0.14 E MJ^{-1} in Q_P/R_S per unit increase of AOD at 500 nm. The ratio Q_P/R_S increases from about 1.82 E MJ^{-1} to about 1.97 E MJ^{-1} when the water vapor content increases from 2 to 10 mm, with the effect diminishing for higher values of water vapor content. The simple all-weather empirically derived model estimates instantaneous Q_P with high accuracy at the site where the model is developed. The mean bias error is close to zero and root mean square error is 3.8%, respectively. Application of the model to data collected from different locations also results in reasonable estimates of Q_P.

1. Introduction

Solar radiation in the 400–700 nm spectral range is called photosynthetically active radiation (PAR) and is one key factor influencing plant physiology, biomass production and natural illumination (Zhou et al., 1996). The following three techniques can be used to measure PAR: (i) integration of spectral irradiance measurements in the 400–700 nm wavelength range using spectroradiometers; (ii) through combined filtered data, i.e., spectral solar irradiance measurements in wavebands 300–2700 nm and 695–2700 nm; and (iii) measurement by means of a quantum sensor (Ross and Sulev, 2000; Jacovides et al., 2004). PAR can be expressed in terms of energy unit (R_P, W m^{-2}) or in photosynthetic photon flux density units (Q_P, μmol m^{-2} s^{-1}). A worldwide network for routinely measuring Q_P has not yet been established, despite the biological importance of this radiometric quantity. Q_P is often calculated as a constant ratio of broadband solar radiation (R_S: 250–5000 nm) (Rao, 1984; Papaioannou et al., 1993). Because cloud amount, water vapor content and aerosol loading can vary from one climatic region to another, a wide range of values for this ratio (Q_P/R_S) has been reported. The ratio is expected to

* *Corresponding author*. Tel.: +86 10 82995071.
E-mail address: xiaxiangao2000@yahoo.com (X. Xia).
0168-1923/$ – see front matter
doi:10.1016/j.agrformet.2008.02.008

increase with water vapor content and cloud amount but decrease with aerosol loading and the solar zenith angle (Jacovides et al., 2004; Papaioannou et al., 1996; Schafer et al., 2002; Zhou et al., 1996). These factors should be considered in order to precisely determine the ratio Q_P/R_S. However, factors such as cloud optical thickness, position relative to the Sun, and liquid/ice water content make it extremely difficult to develop a quantitative relationship between cloudiness and the ratio Q_P/R_S. A few studies describe the estimation of Q_P from some commonly measured or computed quantities, such as the solar zenith angle, sky brightness Δ (the ratio of diffuse irradiance to extraterrestrial irradiance, both on a horizontal surface) and the clearness index K_t (the ratio of R_S to extraterrestrial irradiance, both on a horizontal surface) (Alados et al., 1996; Gonzalez and Calbo, 2002; Jacovides et al., 2003). In addition to their objective nature, these quantities are general indicators of the scattering and absorption processes of all atmospheric constituents, which include aerosols, gases and clouds. Frouin and Pinker (1995) suggested that the spatial and temporal variability of the ratio of PAR to broadband solar radiation, which governs the accuracy of estimates of the former from the latter, warranted further investigation.

The objective of this paper, apart from showing the seasonal variation of Q_P/R_S and the quantitative effects of aerosol loading and water vapor content on Q_P/R_S, is to introduce a simple and efficient parameterization of Q_P using simultaneous measurements of Q_P and R_S taken at a suburban location in northern China. The proposed model is validated using solar radiation data collected at this site. Extension of this model to data from other locations is also evaluated.

1.1. *Site, instruments, and methodology*

The ''East Asian Study of Tropospheric Aerosols: an International Regional Experiment'' (EAST-AIRE) commenced in 2004 with the goal of gaining insight about aerosol properties and their climatic and environmental effects in China (Li et al., 2007a,b). In September 2004, the first EAST-AIRE site was established at Xianghe (39.753°N, 116.961°E, 30 m above sea level), where a set of solar radiometers was installed side-by-side on the roof of a four-story building where the field-of-view is unobstructed in all directions (Xia et al., 2007a). This region experiences a continental monsoon climate commonly found in the temperate zone. In winter, cold, dry winds blow out of Siberia and Mongolia to the northwest; in summer, warm, moist air currents from the southeast take over. The average annual rainfall is about 600 mm with two-thirds of it falling during the summer. Given its location between two megacities (Beijing and Tianjin, 70 km to the northwest and to the southeast, respectively) and depending on the wind direction, the site experiences both natural aerosols and anthropogenic pollutants of urban, rural, or mixed origins. A thick layer of haze often covers the region and aerosol loading and properties show strong day-to-day variations. When dust storms occur during spring period, the aerosol optical depth in the visible can reach more than 3.0 at times (Zhang et al., 2002; Xia et al., 2005).

A CM21 radiometer and a PAR-LITE quantum sensor, both manufactured by Kipp & Zonen (Delft, The Netherlands) were used to measure both global R_S and Q_P. In addition, a set of redundant instruments was installed (another global CM11 radiometer (Delft, The Netherlands), as well as an Eppley normal incidence pyrheliometer and a black & white radiometer (Newport, Rhode Island, USA), both mounted on an EKO STR-22 solar tracker) to ensure the precision of measurements, and also to rule out possible biases due to physical problems (e.g. a misaligned solar shadowing disk). Daily checks were made to ensure that the radiometers were positioned horizontally and that the domes of the radiometers were clean. The data were quality-checked using the Baseline Surface Radiation Network quality control procedure (Ohmura et al., 1998). The instrument sensitivity degradation was monitored via annual comparisons against new or newly calibrated radiometers that were brought to China for establishing new observation sites. The accuracies of global R_S and Q_P are estimated to be about 3% (Long and Ackerman, 2000) and 5% (estimated by the manufacturer), respectively. The daily mean and 5-min means were computed from 1-min raw data to minimize the response time difference between the CM21 and PAR-LITE instruments. More than 3 year's worth of continuous measurements has been collected so far. Radiation data from October 2004 to September 2006 are used in this study. In addition, aerosol optical depths (AOD) were retrieved from spectral extinction measurements obtained by a CIMEL sun/sky radiometer at the Xianghe site. The column-integrated water vapor contents are also derived from measurements made at 940 nm (Holben et al., 1998). These data are available from the Aerosol Robotic Network (AERONET) data pool (http://aeronet.gsfc.nasa.gov). The AOD and water vapor content data are used to study their effects on the ratio Q_P/R_S.

In addition to data collected at Xianghe, measurements of Q_P and R_S from two other sites in China (Liaozhong and Taihu) are also used to provide further assessment of the all-weather model developed for the parameterization of Q_P. Measurements of Q_P and R_S were taken using PAR-LITE and CM21 instruments and daily maintenance was performed at two sites. Data from April to July 2005 at Liaozhong and from September 2005 to August 2006 at Taihu were used in the assessment. The Liaozhong site is located in a suburban region in northeastern China (41°30′N, 120°42′E, 15 m above sea level). In spring, cold and dry currents from the northwest take over this site. A mixture of coarse and fine particles due to anthropogenic activities and dust storms leads to high aerosol optical depth (Xia et al., 2007b). The Taihu site is located in the Yangtze Delta region of China (31°42′N, 120°21′E, 10 m above sea level). The Yangtze Delta experiences a marine monsoon subtropical climate, and the weather is generally warmer and more humid than that in northern China. The region is a key industrial and agricultural area that experiences high aerosol loadings all year round (Xia et al., 2007c). The model performance is evaluated using the methodology recommended by Willmott (1982). An array of complementary difference and summary univariate indices are computed: the mean bias error (MBE), the root mean square error (RMSE), their

systematic and unsystematic proportions or magnitudes ($RMSE_s$ and $RMSE_u$) and the coefficient of determination (R^2). The equations used to calculate these indices are as follows:

$$MBE = N^{-1}\sum(P_i - O_i) \quad (1)$$

$$RMSE = \left[N^{-1}\sum(P_i - O_i)^2\right]^{1/2} \quad (2)$$

$$RMSE_s = \left[N^{-1}\sum(\hat{P}_i - O_i)^2\right]^{1/2} \quad (3)$$

$$RMSE_u = \left[N^{-1}\sum(P_i - \hat{P}_i)^2\right]^{1/2} \quad (4)$$

$$R^2 = \frac{[N\sum P_iO_i - \sum P_i\sum O_i]^2}{[N\sum P_i^2 - (\sum P_i)^2] \times [N\sum O_i{}^2 - (\sum O_i)^2]} \quad (5)$$

where O and P represent observations and predictions of Q_P, respectively, and N is the number of cases. The parameter with a caret symbol is defined as $\hat{P}_i = a + bO_i$, where a and b are the intercept and slope of the least-squares fit between O and P, respectively.

2. Results

2.1. Variability in daily mean Q_P/R_S

It has generally been the practice to express the measured daily, or hourly Q_P as fraction of R_S in order to detect systematic relationships between the two quantities. The daily ratios in this study have been computed by summing the individual quantities over the course of a day, and then taking the ratio of the sums, except when stated otherwise.

Fig. 1 shows box plots of the monthly statistics of Q_P/R_S, AOD at 500 nm, water vapor content and clearness index at Xianghe. Different symbols represent the monthly median, mean, and first and third quartiles. Some features can be seen from the plotted statistics. First, a significant monthly variation in Q_P/R_S is evident. The mean Q_P/R_S gradually increases from about 1.87 E MJ^{-1} in January to about 2.08 E MJ^{-1} in July and then gradually decreases to about 1.89 E MJ^{-1} in December (see also Table 1).

This distinct seasonal variation in Q_P/R_S results from seasonal variations in water vapor content and cloud amount. Under more cloudy and humid conditions, the absorption of solar radiation in the infrared region of the solar spectrum is enhanced, whereas absorption in the PAR spectral region does not vary significantly. Thus, an increase in Q_P/R_S under cloudy

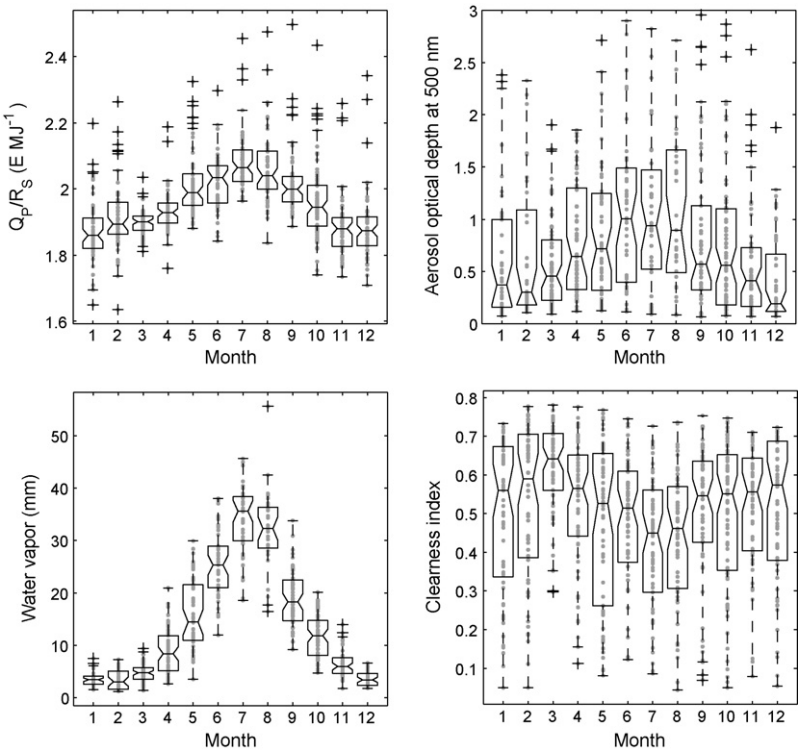

Fig. 1 – Box plots of the monthly ratio of photosynthetic photon flux density to solar radiation (upper left panel); aerosol optical depth at 500 nm (upper right panel); water vapor content (bottom left panel) and clearness index (bottom right panel). In each box, the central bar is the median and the lower and upper limits are the first and the third quartiles, respectively. The lines extending vertically from the box indicate the spread of the distribution with the length being 1.5 times the difference between the first and the third quartiles. Observations falling beyond the limits of those lines are indicated by plus symbols. The black dots indicate geometric means.

Table 1 – Monthly mean and one standard deviation (S.D.) of the ratios of photosynthetic photon flux density to broadband solar radiation (unit: E MJ^{-1}).

Q_P/R_S	January	February	March	April	May	June	July	August	September	October	November	December
Mean	1.87	1.92	1.90	1.94	2.02	2.02	2.08	2.06	2.02	1.96	1.89	1.89
S.D.	0.10	0.11	0.04	0.07	0.10	0.08	0.09	0.11	0.10	0.11	0.10	0.11

skies or humid conditions and a decrease in Q_P/R_S under cloudless skies or dry conditions are expected. Second, there is a wide range in daily values of Q_P/R_S for each month. The monthly difference between the maximum and minimum values of Q_P/R_S (after deleting outliers that are defined to be 1.5 times the difference between the first and third quartiles) ranges from about 0.2 to 0.5 E MJ^{-1}. The lower values of Q_P/R_S occurring in each month are mainly due to heavy aerosol loading. This can be seen from the time series of a pollution event presented in Fig. 2. There was a gradual increase in AOD over a period of 7 days in October 2004. At the beginning of the month, the atmosphere was very clean (AOD ~ 0.1) but over the period of several days, the AOD reached values up to 2.5 E MJ^{-1}. The ratio Q_P/R_S decreased proportionally from about 2.05 E MJ^{-1} (AOD ~ 0.1) to about 1.8 E MJ^{-1} (AOD ~ 2.5) during this time. An even larger decrease in Q_P/R_S would be expected if the water vapor content had remained steady during this period.

2.2. *Effects of aerosol optical depth and water vapor content on Q_P/R_S*

The effect of aerosol loading on the substantial reduction in Q_P/R_S was examined using data from days when the water vapor content ranged from 15 to 20 mm. The increase in Q_P/R_S due to changes in the water vapor content was explored using data from days with low aerosol loading ($0.1 < AOD < 0.2$). The results are presented in Fig. 3.

Note that only measurements made under clear-sky conditions were used to calculate daily Q_P/R_S in order to eliminate the effects of cloud on this ratio. The discrimination of clear skies from cloudy skies was achieved using the empirical clear-sky detection algorithm proposed by Long and Ackerman (2000), with some modifications to better cope with the specific conditions under study (Xia et al., 2007a). Fig. 3 shows that Q_P/R_S decreases linearly with AOD and that 82% of the variability

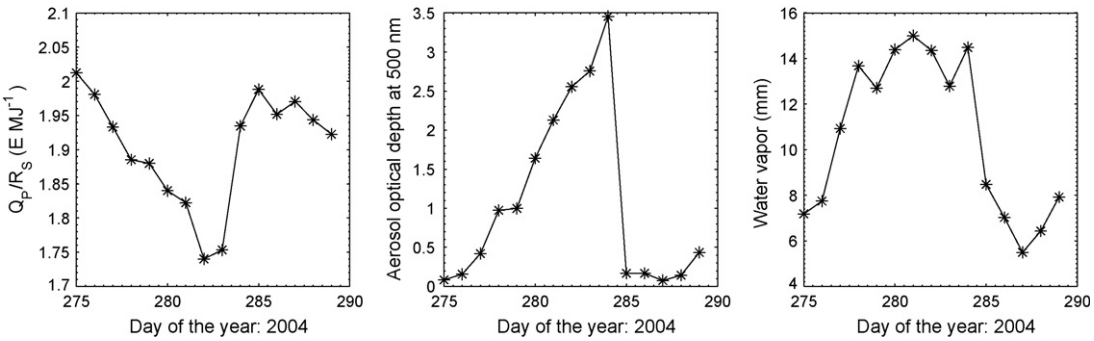

Fig. 2 – Daily mean ratio of photosynthetic photon flux density to global solar radiation (left panel), aerosol optical depth at 500 nm (middle panel) and water vapor content (right panel) during a pollution episode that occurred in northern China from 1–15 October 2004.

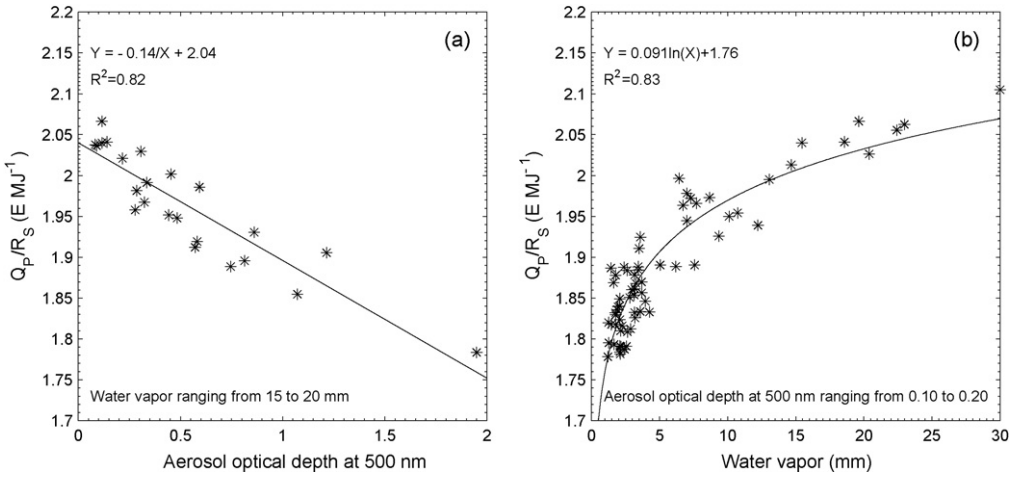

Fig. 3 – Daily mean ratio of photosynthetic photon flux density to broadband solar radiation as a function of daily aerosol optical depth at 500 nm for days with daily water vapor contents ranging from 15 to 20 mm (left panel) and as a function of daily mean water vapor content for days with daily aerosol optical depths at 500 nm ranging from 0.1 to 0.2 (right panel).

Table 2 – Mean ratios of photosynthetic photon flux density to broadband solar radiation obtained at different sites (the values in parentheses represent the range of values)

Ratio (E MJ^{-1})	Location	References
1.92 (1.86–1.94)	Athalassa, Cyprus	Jacovides et al. (2004)
2.08 (1.92–2.14)	Ilorin, Nigeria	Udo and Aro (1999)
1.99	Lusaka, Zambia	Finch et al. (2004)
1.83 (1.77–1.98)	Beijing, China	Hu et al. (2007)
(1.92–2.01)	Chengdu and Kunming, China	Wang and Shui (1990)
2.06	Yucheng, China	Zhou et al. (1996)
1.99	Girona, Spain	Gonzalez and Calbo (2002)
1.94	Naeba Mountain, Japan	Wang et al. (2007)
1.96 (1.87–2.08)	Xianghe, China	This study

in the ratio can be explained by AOD. The resulting regression indicates a reduction of about 0.14 E MJ^{-1} in Q_P/R_S per unit increase in AOD. Schafer et al. (2002) found that smoke aerosols led to a significant reduction in the PAR ratio (~0.13) for each unit increase in AOD. With regard to the water vapor effect, 83% of the variability of the ratio can be explained by the water vapor content in this case. A dependence of the form $Y = 0.091 \ln(X) + 1.76$ was derived. This indicates an increase in Q_P/R_S from 1.82 to 1.97 E MJ^{-1} when the water vapor content increases from 2 to 10 mm. A lower increase is seen for higher values of water vapor content. This increase in Q_P/R_S is larger than that obtained in the Amazon region, where Q_P/R_S increases from about 2.07 to 2.10 E MJ^{-1} when the water vapor content increases from 20 to 30 mm (Schafer et al., 2002). This is expected because the dependence of Q_P/R_S on the water vapor content is not as strong at higher water vapor contents characteristic of the Amazon region.

2.3. Q_P/R_S at Xianghe and published results from other locations

The annual mean Q_P/R_S at Xianghe is 1.96 E MJ^{-1}. Table 2 lists values of Q_P/R_S at other sites around the world. Note that the results from Wang and Shui (1990) and Zhou et al. (1996) are converted from the ratio of PAR energy flux to broadband solar radiation energy (no unit) using the widely used constant of 4.57 μmol photon J^{-1} (McCree, 1972). All results are on a daily time scale and the wavelength range for PAR is 400–700 nm. Table 2 shows that Q_P/R_S varies significantly from site to site. The daily and monthly variability in Q_P/R_S at Xianghe is much larger than that reported by Wang and Shui (1990) at two other sites in China. They stated that within any given season, the ratio did not vary considerably from day to day or from month to month. Even under the influence of clouds, the daily ratio varied slightly. The annual mean value of Q_P/R_S at the Xianghe site is less than that obtained at Yucheng, a suburban region about 400 km south of Xianghe, but is larger than that at Beijing, 70 km away from Xianghe (Hu et al., 2007). This suggests a large spatial variation in Q_P/R_S in northern China.

2.4. The dependence of Q_P on the clearness index

On the basis of 15 month's worth of data at the Xianghe site, an empirical equation was developed to describe the dependence of instantaneous PAR on the cosine of the solar zenith angle (μ) and AOD under cloudless conditions, i.e., $PAR = a_1\mu^{a_2}\exp[a_3\mu^{a_4}AOD]$, where a_i represents four parameters (Xia et al., 2007a). Extension of this equation to data from other locations is restrictive because measurements of AOD are very limited in terms of geography. More importantly, the equation is only suitable for clear-sky conditions. The parameter K_t was chosen here for use in developing a simple all-weather model of Q_P because (1) K_t is a more objective parameter than manual observations of sky cover and (2) K_t is a general indicator of the scattering and absorption processes of all atmospheric constituents.

The 2 year's worth of data used in this study were first divided into two groups: one group for model development, comprised of 75% of all the data (randomly chosen), and another group for validation, comprised of the remainder of the data. Fig. 4 shows Q_P as a function of μ. Different colors represent data with different K_t values. The figure shows that Q_P increases almost exponentially with μ for a specified K_t. Long and Ackerman (2000) suggested using a power law equation to describe the dependence of R_S on μ under clear-sky conditions. The relationship between Q_P and μ for a very narrow range of K_t can also be fit very well using the power law equation:

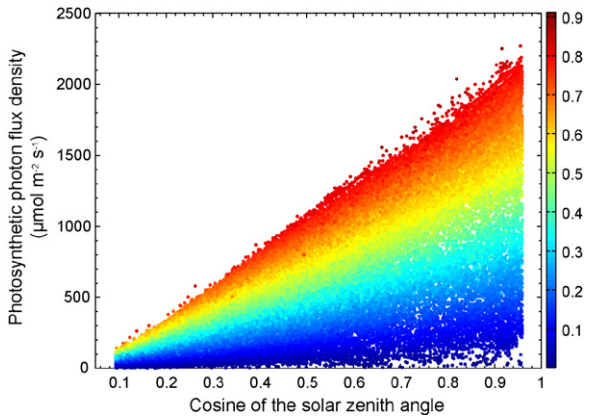

Fig. 4 – Photosynthetic photon flux density as a function of the cosine of the solar zenith angle. Different clearness index (K_t) values are represented by different colors. The values of photosynthetic photon flux density within a narrow range of clearness index values increases almost exponentially with the cosine of the solar zenith angle (For interpretation of the references to color in this figure legend, the reader is referred to the web version of the article.).

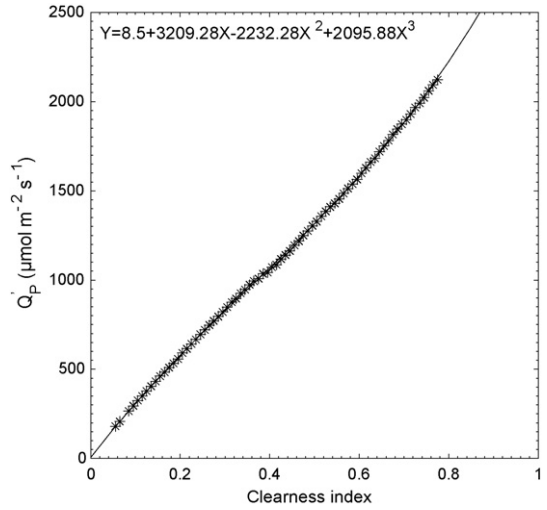

Fig. 5 – The parameter Q'_P as a function of clearness index (K_t), showing the positive correlation between the two variables. The relationship can be expressed as a cubic polynomial equation.

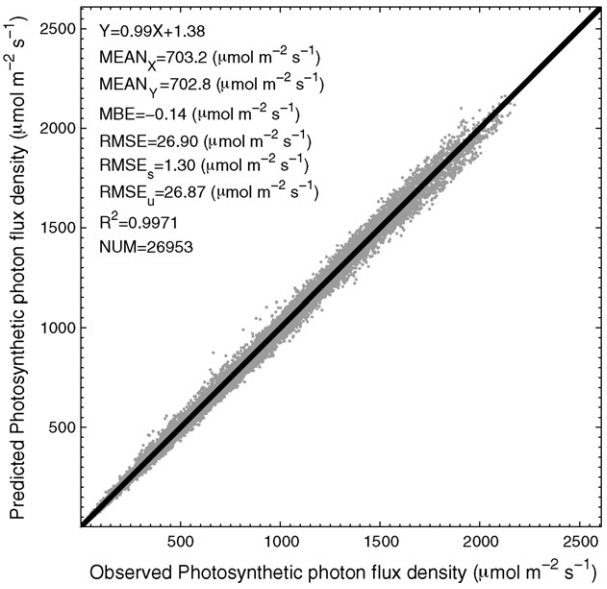

Fig. 6 – Scatterplot of measured photosynthetic photon flux density and the model-predicted values using Eq. (8). The black line represents the 1:1 relationship.

$$Q_P = Q'_P \times \mu^b \quad (6)$$

where Q'_P represents the Q_P for one unit of μ and b determines how Q_P varies with μ. The relationship between Kt and Q_P was explored by first binning K_t values in 0.02 increments starting at 0.01. The data points in each bin were then fit using the power law equation. The resulting regression analyses showed that more than 95% of the variance in Q_P was explained by Eq. (6) and that all relative root mean square errors were less than 5%.

Fig. 5 shows the scatter plot of Q'_P as a function of K_t. The dependence of Q'_P on K_t can be described as follows:

$$Q'_P = 8.5 + 3209.3\,K_t - 2232.3\,K_t^2 + 2095.9\,K_t^3 \quad (7)$$

Although the parameter b from Eq. (6) did not exhibit a clear relationship to K_t, the variation of this parameter was very small and the standard deviation of b was 0.009. Thus, the mean value of this parameter (~1.031) was used. The resulting relative error is about 5% when the solar zenith angle is 80°, which is close to the observation uncertainty. Instantaneous Q_P can thus be estimated using this equation:

$$Q_P = (8.5 + 3209.3\,K_t - 2232.3\,K_t^2 + 2095.9K_t^3) \times \mu^{1.031} \quad (8)$$

Fig. 6 shows the Q_P estimated using Eq. (8) as a function of measurements of Q_P made at the Xianghe site using 25% of the original data reserved for validation purposes. About 78% of the estimates agree with the measurements to within 5%. The MBE is close to zero and the RMSE is about 26.90 μmol m^{-2} s^{-1}. The systematic difference contributed little to the mean square error. These facts suggest that the empirical formulation performs very well and can be used to estimate instantaneous Q_P with high accuracy at the site where the model is developed.

Reliable Q_P predictions were obtained through Eq. (8) by using the two independent data sets performed at the Liaozhong and Taihu sites (Figs. 7 and 8). The relative deviations between the estimates and measurements were less than 5% for 77% of the cases at the Liaozhong site; the MBE and the RMSE were 8.5 and 32.7 μmol m^{-2} s^{-1}, respectively. As regards the model's performance at the Taihu site, the relative differences between observations and predictions were less than 5% for 52% of cases; the MBE and the RMSE were about 2.4 and 3.8%, respectively. A weak model's underestimation is revealed through MBE predictor and regression parameters

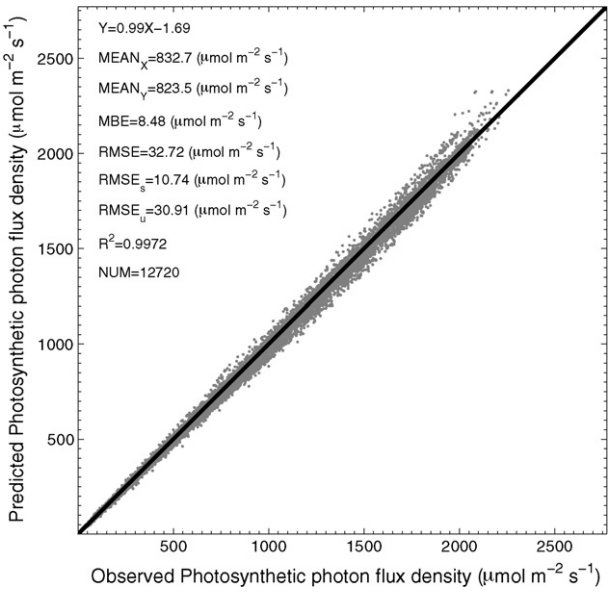

Fig. 7 – As in Fig. 6 but based on measurements from April to July 2005 at the Liaozhong site.

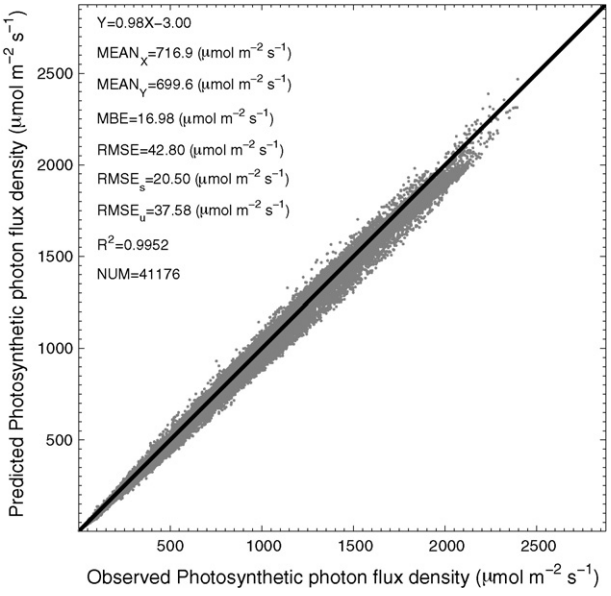

Fig. 8 – As in Fig. 6 but based on measurements from September 2005 to August 2006 at the Taihu site.

(a and b) calculated from the fitting of the data at both sites. The proportion of the difference that arises from systematic errors was only about 10% at Liaozhong and 23% at Taihu. These results suggest that the model provides acceptable estimates of Q_P at locations other than where the relationship was developed. There may be some dependence between the parameters in the model and local climatic factors, which may vary from one geographic area to another, but that particular investigation is out of the scope of this study.

3. Conclusions

Two year's worth of surface radiation data obtained at the Xianghe site in northern China were used to study the ratio of photosynthetic photon flux density to global solar radiation (Q_P/R_S). The monthly variation of this ratio and its dependence on aerosol optical depth and water vapor content were analyzed. An empirical model was developed to describe the dependence of Q_P on the cosine of the solar zenith angle and the clearness index.

The annual mean Q_P/R_S is 1.96 E MJ^{-1}. Q_P/R_S shows a distinct monthly variation, increasing from 1.87 E MJ^{-1} in January to 2.08 E MJ^{-1} in July and then gradually decreasing to 1.89 E MJ^{-1} in December. There is also a significant day-to-day variation in Q_P/R_S for each month. The difference between the maximum and minimum daily values ranges from about 0.2 to 0.5 E MJ^{-1}. Instances when the ratios are low are associated with occurrences of pollution episodes.

The regression relationship between Q_P/R_S and aerosol optical depth indicates that aerosols lead to a reduction of 0.14 E MJ^{-1} in Q_P/R_S for each unit increase in aerosol optical depth. When the aerosol optical depth is low (0.10–0.20), the regression relationship between Q_P/R_S and the water vapor content can be expressed as $Y = 0.091 \ln(X) + 1.76$. This indicates that Q_P/R_S increases from about 1.82 E MJ^{-1} to about 1.97 E MJ^{-1} when the water vapor content increases from 2 to 10 mm. This increase is less pronounced for higher values of water vapor content.

A simple and efficient all-weather model was developed to estimate instantaneous Q_P using two input variables: the cosine of the solar zenith angle and global solar radiation. The cosine of the solar zenith angle is easily calculated and global solar radiation is usually systematically measured at most radiometric stations. The validation analysis shows that the model performs very well at Xianghe and provides very good results when applied to data from two other locations.

Acknowledgements

The research is supported by the Knowledge Innovation Project of the Chinese Academy of Science (IAP07115), the Natural Science Foundation of China (40775009; 40575058), the National Basic Research of China (2006CB403706), and the NASA Radiation Science Program (NNG04GE79G) managed by Dr. Hal Maring.

REFERENCES

Alados, I., Foyo-Moreno, I., Alados-Arboledas, L., 1996. Photosynthetically active radiation: measurements and modeling. Agric. Forest Meteorol. 78, 121–131.

Finch, D.A., Bailey, W.G., McArthur, L.J.B., Nasitwitwi, M., 2004. Photosynthetically active radiation regimes in a southern African savanna environment. Agric. Forest Meteorol. 122, 229–238.

Frouin, R., Pinker, R., 1995. Estimating photosynthetically active radiation (PAR) at the Earth's surface from satellite observations. Remote Sens. Environ. 51, 98–107.

Gonzalez, J.A., Calbo, J., 2002. Modeled and measured ratio of PAR to global radiation under cloudless skies. Agric. Forest Meteorol. 110, 319–325.

Holben, B.N., Eck, T.F., Slutsker, I., Tanre, D., Buis, J.P., Setzer, A., Vermote, E., Reagan, J.A., Kaufman, Y.J., Nakajima, T., Lavenu, F., Jankowiak, I., Smirnov, A., 1998. A federated instrument network and data archive for aerosol characterization. Remote Sens. Environ. 66, 1–16.

Hu, B., Wang, Y., Liu, G., 2007. Measurements and estimations of photosynthetically active radiation in Beijing. Atmos. Res. 85, 361–371.

Jacovides, C.P., Tymvios, F.S., Asimakopoulos, D.N., Theofilou, K.M., Pashiardes, S., 2003. Global photosynthetically active radiation and its relationship with global solar radiation in the Eastern Mediterranean basin. Theor. Appl. Climatol. 48, 23–27.

Jacovides, C.P., Tymvios, F.S., Papaioannou, G., Asimakopoulos, D.N., Theofilou, K.M., 2004. Ratio of PAR to broadband solar radiation measured in Cyprus. Agric. Forest Meteorol. 121, 135–140.

Li, Z., Xia, X., Cribb, M., Mi, W., Holben, B., Wang, P., Chen, H., Tsay, S., Eck, T., Zhao, F., Dutton, E., Dickerson, R., 2007a. Aerosol optical properties and its radiative effects in northern China. J. Geophys. Res. 112, D22S01, doi:10.1029/2006JD007382.

Li, Z., Chen, H., Cribb, M., Dickerson, R., Holben, B., Li, C., Lu, D., Luo, Y., Maring, H., Shi, G., Tsay, S., Wang, P., Wang, Y., Xia, X., Zhao, F., 2007b. Overview of east Asian studies of

tropospheric aerosols, an international regional experiment (EAST-AIRE). J. Geophys. Res. 112, D22S00, doi:10.1029/2007JD008853.

Long, C.N., Ackerman, T.P., 2000. Identification of clear skies from broadband pyranometer measurements and calculation of downwelling shortwave cloud effects. J. Geophys. Res. 105, 15609–15626.

McCree, K.J., 1972. Test of current definitions of photosynthetically active radiation against leaf photosynthesis data. Agric. Meteorol. 10, 443–453.

Ohmura, A., Gilgen, H., Hegner, H., Muller, G., Wild, M., Dutton, E.G., Forgan, B., Frohlich, C., Philipona, R., Heimo, A., Langlo, G.K., McArthur, B., Pinker, R., Whitlock, C., Dehne, K., 1998. Baseline surface radiation network (BSRN/WCRP): new precision radiometry for climate research. Bull. Am. Meteorol. Soc. 79, 2115–2136.

Papaioannou, G., Papanikolaou, N., Retails, D., 1993. Relationships of photosynthetically-active radiation and shortwave irradiance. Theor. Appl. Climatol. 48, 23–27.

Papaioannou, G., Nikolidakis, G., Asimakopolos, D., Retails, D., 1996. Photosynthetically-active radiation in Athens. Agric. Forest Meteorol. 81, 287–298.

Rao, C.R.N., 1984. Photosynthetically active components of global solar radiation: measurements and model computations. Arch. Meteorol. Geophys. Bioclim. 34, 353–364.

Ross, J., Sulev, M., 2000. Sources of errors in measurements of PAR. Agric. Forest Meteorol. 100, 103–125.

Schafer, J.S., Holben, B.N., Eck, T., Yamasoe, M., Araxo, P., 2002. Atmospheric effects on insolation in the Brazilian Amazon: observed modification of solar radiation by clouds and smoke and derived single scattering albedo of fire aerosols. J. Geophys. Res. 107 , doi:10.1029/2001JD00428.

Udo, S.O., Aro, T.O., 1999. Global PAR related to global solar radiation for central Nigeria. Agric. Forest Meteorol. 97, 21–31.

Wang, B., Shui, Y., 1990. The latest test results of photosynthetically active radiation. Q. J. Appl. Meteorol. 1, 185–190 (in Chinese).

Wang, Q., Kakubari, Y., Kubota, M., Tenhunen, J., 2007. Variation of PAR to global solar radiation ratio along altitude gradient in Naeba Mountain. Theor. Appl. Climatol. 87, 239–253.

Willmott, C.J., 1982. Some comments on the evaluation of model performance. Bull. Am. Meteorol. Soc. 11, 1309–1313.

Xia, X., Chen, H., Wang, P., Zong, X., Qiu, J., Goloub, P., 2005. Aerosol properties and their spatial and temporal variations over North China in spring 2001. Tellus 57b, 28–39.

Xia, X., Li, Z., Wang, P., Chen, H., Cribb, M., 2007a. Estimation of aerosol effects on surface irradiance based on measurements and radiative transfer model simulations in northern China. J. Geophys. Res. 112, D22S10, doi:10.1029/2006JD008337.

Xia, X., Chen, H., Li, Z., Wang, P., Wang, J., 2007b. Significant reduction of surface solar irradiance induced by aerosols in a suburban region in northeastern China. J. Geophys. Res. 112, D22S02, doi:10.1029/2006JD007562.

Xia, X., Li, Z., Holben, B., Wang, P., Eck, T., Chen, H., Cribb, M., Zhao, Y., 2007c. Aerosol optical properties and radiative effects in the Yangtze Delta region of China. J. Geophys. Res. 112, D22S12, doi:10.1029/2007JD008859.

Zhang, W., Lu, D., Wang, P., 2002. The observation and analysis of atmospheric aerosol optical thickness over Beijing area. China Environ. Sci. 22, 495–500 (in Chinese).

Zhou, Y., Xiang, Y., Luan, L., 1996. Climatological estimation of quantum flux densities. Acta Meteorol. Sin. 54, 447–455 (in Chinese).